Coupled Systems Mechanics, *Vol. 10, No. 1 (2021) 79-102*
DOI: https://doi.org/10.12989/csm.2021.10.1.079

Linearized instability analysis of frame structures under non-conservative loads: Static and dynamic approach

Emina Hajdo*[1], Rosa Adela Mejia-Nava[2], Ismar Imamovic[1] and Adnan Ibrahimbegovic[2,3]

[1]Faculty of Civil Engineering, University of Sarajevo, Patriotske lige 30, Sarajevo, BiH, Bosnia and Herzegovina
[2]Université de Technologie Compiégne, Laboratoire Roberval de Mécanique, Rue du Dr Schweitzer, 60200 Compiègne, France
[3]Institut Universitaire de France, France

(Received November 27, 2020, Revised December 12, 2020, Accepted January 18, 2021)

Abstract. In this paper we deal with instability problems of structures under nonconservative loading. It is shown that such class of problems should be analyzed in dynamics framework. Next to analytic solutions, provided for several simple problems, we show how to obtain the numerical solutions to more complex problems in efficient manner by using the finite element method. In particular, the numerical solution is obtained by using a modified Euler-Bernoulli beam finite element that includes the von Karman (virtual) strain in order to capture linearized instabilities (or Euler buckling). We next generalize the numerical solution to instability problems that include shear deformation by using the Timoshenko beam finite element. The proposed numerical beam models are validated against the corresponding analytic solutions.

Keywords: instability problems; non-conservative load; Euler-Bernoulli beam; von Karman strain; Timoshenko beam; shear deformation

1. Introduction

Modern urban architecture trends are geared towards constructing tall structures, with either office/residential buildings or transport infrastructure. At the same time, the progress in material engineering that allows to increase the load-bearing capacity and safety of the structure, results with lightweight and slender structural elements for high-rise structures, which all became a symbol of modern engineering. However, by pushing the boundaries of engineering in the aforementioned way, and by designing slender and lightweight structures can result in fatal consequences of loss in structural stability. Namely, the instability phenomena imply that for the reduced structural stiffness at so-called critical equilibrium state, even a small perturbation can lead to a disproportional increase in response (displacement, strain and stress) and eventual structural failures (e.g., see illustrative damage cases for recent US storm Laura url: https://www.fox23.com/news/photos-hurricane/KCGRTCQ4LFFNDHZLW2O6LEE26I/). Thus, the analysis of complex structures

*Corresponding author, Assistant Professor, E-mail: emina.hajdo@gmail.com

http://www.techno-press.org/?journal=csm&subpage=8 ISSN: 2234-2184 (Print), 2234-2192 (Online)

instability, and adequate prevention of its occurrence, has again become one of the fundamental problems faced by engineers. Furthermore, different types of structures, next to (permanent) gravitational forces, are also subjected to various loads. In general, all the forces that act upon the structure can be classified in two categories: conservative and non-conservative. For the conservative forces (e.g., gravitational force), the external work does not depend on the path but only on the starting and ending point. Therefore, the conservative force can be obtained from a potential (e.g., gravity potential) and thus the total work done by a conservative force on a closed path is equal to zero. The forces attributed to external actions (e.g., wind or fluid flow, or yet a frictional force) are often non-conservative (Sugiyama *et al*. 2019). The work of nonconservative forces cannot be computed from a potential, and it depends on the path taken. It is a fundamental finding of Bolotin (1964) that the structure instability under non-conservative forces may occur dynamically, leading to increasing vibration amplitudes (yet called flutter instability). Therefore, the problem of structural instability under non-conservative forces should be examined within the dynamics framework.

Vast majority of analytic solutions is already available (Hajdo *et al*. 2020, Bolotin 1963, Lacarbonara and Yabuno 2006, Jeronen and Kouhia 2015) for the classical problems of a column buckling under non-conservative load. This kind of non-conservative force is also called a follower force (Timoshenko and Gere 1961, Langthjem and Sugiyama 2000, Beck 1952, Farhat *et al*. 2013, McHugh and Dowell 2020). Follower forces depend on the deformation of structures. Namely, these forces follow the structure motion (e.g., cross-section rotation), and are thus path-dependent and not possible to derive from a potential (Sugiyama *et al*. 2019). The stability analysis of such a column under follower force cannot be obtained by using the statics approach of studying the critical equilibrium state (Ibrahimbegovic *et al*. 2013, Hajdo *et al*. 2020, Imamovic *et al*. 2019), but requires using the dynamics framework. Moreover, the stability analysis of such column cannot be placed within the classical Lyapunov stability framework of dynamic motion (Mejia Nava *et al*. 2020, Lozano *et al*. 2000), which pertains to variations of the total energy (Lyapunov functional in Mechanics), simply because no such potential can be established for non-conservative forces.

We propose in this work an original approach of "dynamic" equilibrium equations, where the structure stability can be confirmed by proportionally small vibrations due to small perturbations from its equilibrium position. Such theory of the dynamic instability can be explained by using an example of the column under compressive axial follower force. If such a force is smaller than the Bolotin critical force value, the column response will remain proportionally small due to a small perturbation. However, for the applied force equal or larger than critical, relation between a small perturbation and structure response will become disproportionally large, followed by large vibration amplitudes, which are rapidly increasing (Bolotin 1964). A previous study of Bolotin (1963) was the first to give the analytic solution to elastic column instability problem under non-conservative axial loads. Similar studies of simple structures can also be found in (Timoshenko and Gere 1961), or in a recent survey paper (Langthjem and Sugiyama 2000), for different kinds of columns (Beck's, Reut's etc.) under non-conservative follower loads. These and other works (Jeronen and Kouhia 2015, Beck 1952, Farhat *et al*. 2013, McHugh and Dowell 2020), exploring effects of damping, flutter instability of aircraft wings or columns subjected to rocket thrust, mostly put the emphasis on either analytic solutions or their experimental validations. The study of large beam deflections under conservative and non-conservative load, in static framework can be found in (e.g., Masjedi and Ovesy 2015). Dynamic instability of geometrically exact beams under a follower force using fully intrinsic equations was subject of research in (e.g., Amoozgar and Shahverdi 2016). Many researchers studied follower force as a distributed load (e.g., Fazelzadeh *et al*. 2017). A uniform

cantilever beam subjected to a partially follower load and analyzed using finite element method is presented in (Gasparini *et al*. 1994). A detailed review of papers that deal with the topic of dynamic stability of the structures under follower force can be found in (Elishakoff 2005). The main thrust in this work is directed towards a complementary approach based upon numerical modeling by using the finite element method (Ibrahimbegovic 2009).

In particular, as the first novelty, we introduce the Euler-Bernoulli beam finite element that can deal with instability problems under non-conservative follower force. This is achieved by using the von Karman virtual strain measure, typical of moderate rotations, which can account for instability phenomena within the framework of weak form of instability problem. Some previous studies included the von Karman virtual strain to capture the buckling of frames (e.g., Dujc *et al*. 2010, Piculin and Brank 2015). In our previous work (Ibrahimbegovic *et al*. 2013, Hajdo *et al*. 2020), the von Karman strain was used to formulate the structure instability problem as corresponding linear buckling problem, which reduces to solving the linear eigenvalue problem to predict the critical load for conservative (quasi-static) forces. For the instability problems under non-conservative force studied herein, we also introduce the novelty of adapting the beam element for use in the dynamics framework, and obtain the corresponding dynamic equilibrium solution by employing the Newmark time-integration scheme. The final novelty in this paper is in adapting the proposed approach also to shear deformable beams, with the equivalent of Timoshenko beam model. Some background material and more details needed to master the numerical models developed in this research can be found in our previous work (Ibrahimbegovic *et al*. 2013, Hajdo *et al*. 2020, Imamovic et al. 2019, Mejia Nava *et al*. 2020, Ibrahimbegovic 2009, Medic *et al*. 2013).

The outline of our paper is as follows. In Section 2, we present analytic solutions (based upon the strong form) for a cantilever beam under fixed and follower force, as well as semi-analytic solution for static and dynamic instability of frame structure. The discrete approximation is constructed by FEM as shown in Section 3. In Section 4 we give several illustration examples, and in Section 5 we state conclusions.

2. Strong form based analytic solution

In this section we briefly discuss the analytic solutions for instability of a compressed cantilever under fixed and under follower force. The latter case was first solved by Bolotin (1963), with the analytic solution satisfying all three fundamental equations of the strong form. We then provide the solution for a shear deformable beam, where the Timoshenko rather than the Euler-Bernoulli beam model was used. We finally provide an extension of such solution to instability of frame structure, in terms of semi-analytic solution.

2.1 Cantilever beam instability under fixed load - analytic solution

The analytic solution presented in this section, based upon strong form of Euler-Bernoulli beam, verifying the equations of kinematics, constitutive law and equilibrium. The first two are borrowed from linear beam theory.

1. Kinematics (see Fig. 1(b))

$$\left.\begin{aligned} u^p(x,y) &= -y\cdot\theta = -y\frac{dv(x)}{dx} \\ v^p(x,y) &= v(x) \end{aligned}\right\} \Rightarrow \varepsilon_{xx}^p(x,y) = \frac{du^p}{dx} = -y\frac{d^2v^p}{dx^2} \tag{1}$$

2. Constitutive law

$$\sigma_{xx}(x,y) = E\varepsilon_{xx}(x,y) = -Ey\frac{d^2v^p}{dx^2}$$
$$M = -\int_A y\sigma_{xx}dA = Eb\int_{-h/2}^{h/2} y^2dy = E\frac{bh^3}{12}\frac{d^2v(x)}{dx^2} = EI\frac{d^2v(x)}{dx^2} \tag{2}$$

where b and h are the cross section width and height respectively, M is a bending moment, E modulus of elasticity and I is a moment of inertia. Eq. (2) only holds for rectangular cross-sections. However, the last equation takes into account nonlinearity to establish equilibrium in the deformed configuration, i.e., on the beam deformed axis:

3. Equilibrium:

$$0 = \sum F_y = -\mathcal{V}(x) + \underbrace{T(x+dx)}_{\mathcal{V}(x)+\frac{dT(x)}{dx}dx} + q(x)dx = \frac{dT(x)}{dx} + q(x)$$

$$0 = \sum M = -\mathrm{M}(x) + \underbrace{M(x+dx)}_{M(x)+\frac{dM(x)}{dx}dx+0(dx)} - q(x)dx\frac{dx}{2} + T(x)dx + P\frac{dv}{dx}dx \tag{3}$$

$$= \frac{dM(x)}{dx} + T(x) + P\frac{dv}{dx}$$

$$\frac{d^4M(x)}{dx^4} + P\frac{d^2v(x)}{dx^2} = q(x)$$
$$\frac{d^4v(x)}{dx^4} + \frac{P}{EI}\frac{d^2v(x)}{dx^2} = \frac{q(x)}{EI} \tag{4}$$

were T is a shear force, q is a transverse distributed load. Thus, we are interested in the class of problems known as linearized instability or Euler buckling, which considers small deformations with moderate rotations before reaching the critical equilibrium state. By combining these three equations we obtain the strong form of the problem for Euler buckling

$$\frac{d^4v(x)}{dx^4} + k^2\frac{d^2v(x)}{dx^2} = 0 \quad ; \quad k = \sqrt{\frac{P}{EI}} \tag{5}$$

The general solution for such equation can be written as

$$v(x) = A_1 \sin kx + A_2 \cos kx + A_3 x + A_4 \tag{6}$$

where A_1, A_2, A_3 and A_4 are constants to be obtained from boundary conditions.

The boundary conditions for cantilever beam in Fig. 1 can be written as

$$v(0) = 0 \quad ; \quad M(l) = EI\frac{d^2v(l)}{dx^2} = 0$$
$$\frac{dv(0)}{dx} = 0 \quad ; \quad T(l) = -EI\frac{d^3v(l)}{dx^3} - P\frac{dv(l)}{dx} = 0 \quad \rightarrow \quad k^2\frac{dv(l)}{dx} + \frac{d^3v(l)}{dx^3} = 0 \tag{7}$$

By combining relations in Eqs. (6)-(7), we further obtain

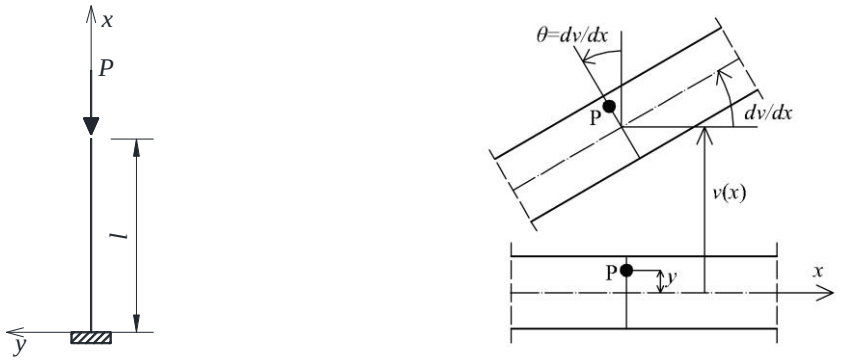

(a) Initial configuration (b) Deformed beam axis

Fig. 1 Linear instability of cantilever

$$\left|\begin{array}{c} v(0)=0 \\ \dfrac{dv(0)}{dx}=0 \\ \dfrac{d^2v(l)}{dx^2}=0 \\ k^2\dfrac{dv(l)}{dx}+\dfrac{d^3v(l)}{dx^3}=0 \end{array}\right. \Rightarrow \underbrace{\begin{bmatrix} 0 & 1 & 0 & 1 \\ k & 0 & 1 & 0 \\ -k^2\sin kl & -k^2\cos kl & 0 & 0 \\ 0 & 0 & k^2 & 0 \end{bmatrix}}_{det[\bullet]=0} \begin{bmatrix} A_1 \\ A_2 \\ A_3 \\ A_4 \end{bmatrix} = \begin{bmatrix} 0 \\ 0 \\ 0 \\ 0 \end{bmatrix} \tag{8}$$

From the above determinant it follows that

$$k^2\cos kl=0 \quad \Rightarrow \quad \cos kl=0 \quad \Rightarrow \quad kl=\frac{2n-1}{2}\pi \ , \ n=1,2,... \tag{9}$$

If we recall the relation for k given in Eq. (5), further we get

$$\frac{P}{EI}=k^2=\frac{(2n-1)^2}{4l^2}\pi^2 \quad \Rightarrow \quad P=\frac{(2n-1)^2\pi^2 EI}{4l^2} \tag{10}$$

Finally, the value of the critical force for Euler's buckling of cantilever beam is

$$P_{cr}=\frac{\pi^2 EI}{(2l)^2} \tag{11}$$

while buckling modes are described with

$$\Phi_n(x)=-\cos\frac{(2n-1)\pi x}{2l}+1 \tag{12}$$

The first buckling mode corresponding to the smallest value of the critical load in Eq. (11) is

$$\Phi_1(x)=1-\cos\frac{\pi x}{2l} \tag{13}$$

In the reminder of this section we extend this analytic solution to the case of shear deformable beam, represented by Timoshenko beam model (see Fig. 2).

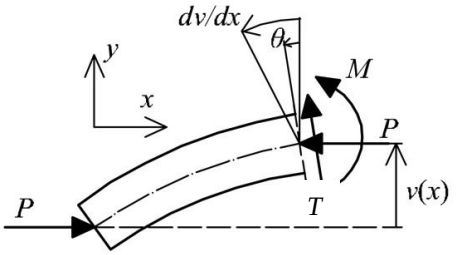

Fig. 2 Deformed configuration of an axially compressed Timoshenko cantilever beam

In the same manner we can now obtain the critical force value for Timoshenko beam as the solution of the strong form combining three fundamental equations: kinematics, constitutive equations and equilibrium. The kinematics of the Timoshenko beam is given as

$$\kappa = \frac{d\theta}{dx} \quad ; \quad \gamma = \frac{dv}{dx} - \theta \tag{14}$$

where θ is independent rotation filed that describes the cross-section position, resulting with new definition of bending κ and shear strain γ.

The corresponding expression for bending moment M and shear force T can be written from constitutive equations as

$$M = (EI)\kappa \quad ; \quad T = (GA)\gamma \tag{15}$$

where G is a shear modulus and A is a cross-sectional area. According to the Fig. 2, the equilibrium on the deformed configuration results in

$$M = -P \cdot v \quad ; \quad T = P \underset{\theta}{\sin\theta} = P\theta \tag{16}$$

Further, by combining the results obtained in Eqs. (14)-(16) we can obtain the relation between the section rotation and beam transverse displacement

$$\begin{aligned} \frac{dv}{dx} &= \theta + \frac{P\theta}{GA} \\ \frac{d^2v}{dx^2} &= \left(1 + \frac{P}{GA}\right)\frac{d\theta}{dx} \end{aligned} \tag{17}$$

With this result in hand, the first relation given in the Eq. (15) can be written

$$\begin{aligned} EI\frac{d\theta}{dx} + P \cdot v &= 0 \\ EI\frac{d^2v}{dx^2}\frac{1}{1+\frac{P}{GA}} + Pv &= 0 \end{aligned} \tag{18}$$

Finally, the differential equation expressing the strong form of instability condition, of the axially compressed Timoshenko beam is given as

$$\frac{d^2v}{dx^2} + \frac{P}{EI}\left(1 + \frac{P}{GA}\right)v = 0 \tag{19}$$

Previous equation can be rewritten in the same format as the one for Euler- Bernoulli beam but by introducing a new definition of the parameter k

$$\frac{d^4v}{dx^4}+k^2\frac{d^2v}{dx^2}=0 \quad ; \quad k=\sqrt{\frac{P(1+P/GA)}{EI}} \tag{20}$$

The general solution of this differential equation can again be written as

$$v(x)=A_1\sin kx+A_2\cos kx+A_3x+A_4 \tag{21}$$

where A_1, A_2, A_3 and A_4 are constants to be determined by taking into account the boundary conditions

$$v(0)=v(l)=0 \quad , \quad M(l)=0 \quad , \quad T(l)=0 \tag{22}$$

Of particular interest is in a nontrivial solution, which is obtained for the case when

$$\cos kl=0 \quad \Rightarrow \quad kl=\frac{2n-1}{2}\pi \qquad n=1,2,... \tag{23}$$

The smallest value of factor k corresponding to the critical force value is computed for n=1. With the last result in hand, by using the relation given in Eq. (19), we get

$$k_{cr}=\frac{\pi}{2l} \quad \Rightarrow \quad P_{cr}\left(1+\frac{P_{cr}}{GA}\right)=\frac{EI\pi^2}{4l^2} \tag{24}$$

By using the last expression, the critical force for Timoshenko beam is obtained as

$$P_{cr}=\frac{\pi^2EI}{2l^2}\frac{1}{1+\sqrt{1+\frac{\pi^2EI}{l^2GA}}} \tag{25}$$

It is obvious that the critical force value computed for Timoshenko beam is smaller than the one obtained for the Euler beam, and when $\gamma\to 0$, $GA\to\infty$, $P_{cr}\to\frac{\pi^2EI}{4l^2}$. This finding is in agreement with Cauchy interlace theorem (e.g., Ibrahimbegovic 2009) since the Timoshenko beam model allows for more deformation modes than the Euler beam model.

2.2 Dynamics framework for instability problems

It was first shown by Bolotin (1964, 1963) that the same procedure no longer works when we have the follower force. In such a case we have to place the instability problem within the dynamics framework. Namely, we now consider a deformed configuration of a beam under compressive axial force P, which undergoes vibrations that should be examined within the dynamics framework.

2.2.1 Cantilever beam analytic solution for thin beams by Bolotin

In this section we present the solution to the problem of instability of the Euler-Bernoulli beam with a concentrated mass on top under the action of a compressive follower force. This implies that the force rotates together with the free end section of the beam and remains tangential to its deformed axis (see Fig. 3).

The analysis of this problem is again carried out under hypothesis of linear kinematics and linear

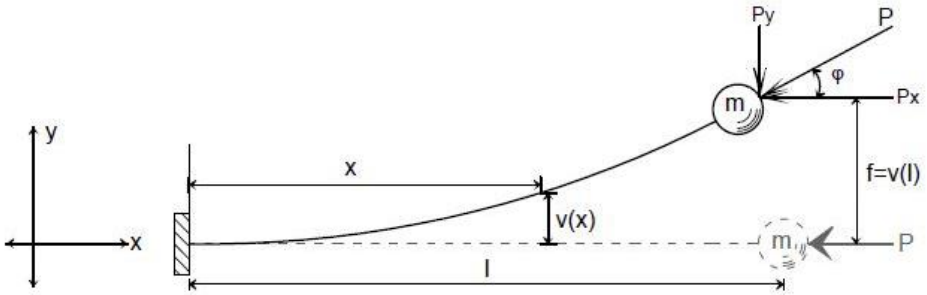

Fig. 3 Euler-Bernoulli cantilever beam under follower load

constitutive equation

$$\varepsilon(x,y) = -y^2 \frac{d^2v}{dx^2} \quad ; \quad \sigma = E\varepsilon \rightarrow M = EI\frac{d^2v}{dx^2} \tag{26}$$

The only nonlinear equation in this instability problem pertains to equilibrium, first assumed as static, which applies in the deformed configuration (indicated by a curved solid line in Fig. 3 above). If we assume small deflection and small end rotation with

$$\varphi = \frac{dv}{dx} << 1 \tag{27}$$

the follower force can be discomposed into horizontal and vertical components with: $P_x \approx P$, $P_y \approx P\varphi$. The moment equation of the (slightly) bent beam is given in (Bolotin 1963)

$$EI\frac{d^2v}{dx^2} = P(f - v) - P\varphi(l - x) \tag{28}$$

where *EI* is the beam bending stiffness, $f=v(l)$ is the deflection at the free end of the beam and l its length. We can propose the general solution of this differential equation as

$$v(x) = A_1 \sin kx + A_2 \cos kx + f - \varphi(1 - x) \tag{29}$$

where A_1 and A_2 are arbitrary constants, whereas f and φ denote free end displacement and rotation.

The boundary conditions for this problem are zero displacement and zero slope at cantilever beam support point and assumed values of displacement and slope at the free end with

$$v(0) = 0 \ , \quad \frac{dv(0)}{dx} = 0 \ , \quad v(l) = f \ , \quad \frac{dv(l)}{dx} = \varphi \tag{30}$$

If we substitute the general solution into these boundary conditions, we obtain the following set of algebraic equations, written in the matrix notation:

$$\begin{bmatrix} 0 & 1 & 1 & -1 \\ k & 0 & 0 & 1 \\ \sin kl & \cos kl & 0 & 0 \\ \cos kl & -\sin kl & 0 & 0 \end{bmatrix} \begin{bmatrix} A_1 \\ A_2 \\ f \\ \varphi \end{bmatrix} = \begin{bmatrix} 0 \\ 0 \\ 0 \\ 0 \end{bmatrix} \tag{31}$$

It is easy to check that the determinant of this matrix is equal to -1, which means that there are no other solutions but trivial, i.e., ($v(x) \cong 0$). Hence, we conclude that the static approach cannot be used to solve this instability problem.

For that reason, we must turn towards finding the solution of such instability problem within the dynamics framework. In other words, we study the possibility of flutter instability. Here, the equilibrium is said to be unstable if a small disturbance causes a large deviation of the system from the considered dynamic equilibrium. With the follower (non-conservative) load explicitly dependent on time, the equation of motion with small oscillations around equilibrium state takes the following form

$$EI\frac{d^2v(x,t)}{dx^2} = P\big(f(t) - v(x,t)\big) - P\varphi(t)(l-x) - m(l-x)\frac{d^2f(t)}{dt^2} \tag{32}$$

where $v(x,t)$ is the dynamic deflection at each point and $f(t)$ is the deflection at the free-end of the cantilever, i.e., $f(t)=v(l,t)$. The solution to this equation can be obtained by separation of variables

$$v(x,t) = \upsilon(x)e^{i\omega t}\ ,\quad f(t) = fe^{i\omega t}\ ,\quad \varphi(t) = \phi e^{i\omega t} \tag{33}$$

where we can assume that the beam performs free vibrations with frequency ω. We can thus reduce the Eq. (32) to the form

$$EI\frac{d^2\upsilon}{dx^2} + k^2\upsilon = k^2P - k^2\phi(l-x) + \frac{m\omega^2 f}{EI}(l-x) \tag{34}$$

The general solution of the last equation can be written as

$$\upsilon(x) = A_1 \sin kx + A_2 \cos kx + f - \phi(l-x) + \frac{m\omega^2 f}{k^2EI}(l-x) \tag{35}$$

Making use of the corresponding boundary conditions for cantilever beam $v(0)=0$, $v'(0)=0$, $v(l)=f$, $v'(l)=\phi$, we obtain a new form of the system in Eq. (31), and again check for non-trivial solutions by enforcing that

$$\begin{bmatrix} 0 & 1 & 1+\dfrac{m\omega^2 l}{k^2EI} & -l \\ k & 0 & -\dfrac{m\omega^2}{k^2EI} & 1 \\ \sin(kl) & \cos(kl) & 0 & 0 \\ k\cos(kl) & -k\sin(kl) & -\dfrac{m\omega^2}{k^2EI} & 0 \end{bmatrix} = 0 \tag{36}$$

We can further obtain the corresponding value of ω from zero determinant condition in Eq. (36) above, and find out that such value becomes infinite (non-physical) if the following condition is verified

$$\omega = \pm\sqrt{\frac{P}{ml}\frac{1}{\dfrac{\sin kl}{kl} - \cos kl}} \ \to \infty \ \Leftrightarrow \ \tan kl = kl \tag{37}$$

The last expression provides the numerical solution for the critical value $kl = \sqrt{2.05}\pi$. Thus, the critical follower load for Euler-Bernoulli beam can be computed as

$$k = \sqrt{\frac{P}{EI}} \;\rightarrow\; P_{cr} = \frac{2.05\pi^2}{l^2} EI \tag{38}$$

If we now have a cantilever beam with the distributed mass (see Fig. 4) the beam motion is governed by

$$EI\frac{d^4v}{dx^4} + P\frac{d^2v}{dx^2} + m\frac{d^2v}{dt^2} = 0 \quad \Leftrightarrow \quad \frac{d^4v}{dx^4} + k^2\frac{d^2v}{dx^2} + \omega^2\frac{d^2v}{dt^2} = 0 \tag{39}$$

The boundary conditions at the fixed end and at the free end of cantilever are given as:

$$v(0,t) = \frac{\partial v(0,t)}{\partial x} = 0 \quad ; \quad \frac{\partial^2 v(l,t)}{\partial x^2} = \frac{\partial^3 v(l,t)}{\partial x^3} = 0 \tag{40}$$

Furthermore, we can rewrite the differential equation of the free vibrations of the column as follows

$$\frac{d^4g}{dx^4} + k^2\frac{d^2g}{dx^2} - \frac{m\omega^2}{EI}g = 0 \tag{41}$$

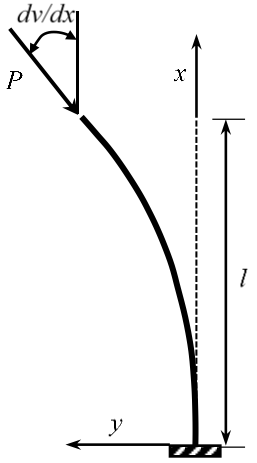

Fig. 4 Beck's column under a follower force

The general solution of the differential equation is given with

$$g(x) = B_1 \sin\alpha x + B_2 \cos\alpha x + B_3 \sinh\beta x + B_4 \cosh\beta x \tag{42}$$

where α and β are

$$\alpha = \frac{k}{\sqrt{2}}\left(1 + \sqrt{1 + \frac{4m\omega^2}{EIk^4}}\right)^{1/2} \quad ; \quad \beta = \frac{k}{\sqrt{2}}\left(-1 + \sqrt{1 + \frac{4m\omega^2}{EIk^4}}\right)^{1/2} \tag{43}$$

By taking into account the boundary conditions, and searching for the nontrivial solution, we obtain the critical force value as follows

$$P_{cr} = \frac{2\pi^2 EI}{l^2} \tag{44}$$

2.2.2 Analytic solution for Timoshenko beam buckling under follower force

The instability problem for Timoshenko beam buckling can be defined in a similar manner, by using linear kinematics and constitutive equations, combined with nonlinear equilibrium equation imposed in Timoshenko beam deformed configuration. We have already written all governing equations for the Timoshenko beam instability in Eqs. (14)-(24). We have shown the equivalence of the differential equation governing the instability problem for Timoshenko beam, but with different value of *k*. Hence, the solution to such instability problem will again be computed within the dynamics framework. One can follow the same steps to arrive at the same final result as the one in Eq. (37), but with different value of *k*. Such an approach can now provide the critical value of the follower load for Timoshenko beam, by imposing that

$$k = \sqrt{\frac{P\left(1+\frac{P}{GA_c}\right)}{EI}} \rightarrow k^2 = \frac{2.05\pi^2}{l^2} \tag{45}$$

$$P_{cr} = \frac{\sqrt{1+4\frac{2.05\pi^2 EI}{GA_c}}-1}{\frac{2}{GA_c}} \tag{46}$$

2.3 Static and dynamic instability of frame: semi-analytic solution

In this section we give an analytic solution for the critical load of a frame under two conservative loads applied at the corner nodes. The frame geometry is as shown in Fig. 5.

Under the applied loads, we will have the deformed configuration of the beam as shown in Fig. 6(a). The main idea for constructing the solution is to propose an equivalent system that would have the same deformed shape. Such an equivalent system consists of a cantilever beam with a rotational spring at the free end of the beam, which is an approximate replacement for the restraining beam

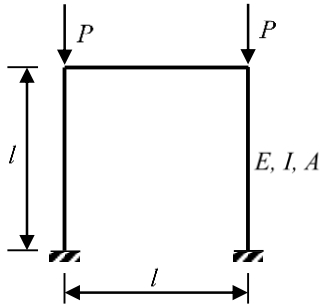

Fig. 5 Frame instability under conservative load

(a) Deformed shape (b) Equivalent system for the frame

Fig. 6 Frame under conservative load

action upon the column (see Fig. 6(b)).

The corresponding differential equation characterizing critical equilibrium state for this problem is similar to the one in Eq. (5) for a cantilever beam

$$\frac{d^4v}{dx^4}+k^2\frac{d^2v}{dx^2}=0 \quad ; \quad k=\sqrt{\frac{P}{EI}} \tag{47}$$

The general solution to this differential equation can be written as follows

$$v(x)=A_1\sin kx+A_2\cos kx+A_3x+A_4 \tag{48}$$

The main modification from the previously developed analytic solution by Bolotin for cantilever beam is a new form of the boundary condition of top of the column, which is brought by the presence of the spring. Thus, we can write as follows

$$v(0)=0 \tag{49}$$

$$\frac{dv}{dx}(0)=0 \tag{50}$$

$$EI\frac{d^2v(l)}{dx^2}+\alpha\frac{dv(l)}{dx}=0 \quad ; \quad \frac{d^2v(l)}{dx^2}+\beta\frac{dv(l)}{dx}=0 \quad ; \quad \beta=\frac{\alpha}{EI} \tag{51}$$

$$EI\frac{d^3v(l)}{dx^3}+P\frac{dv(l)}{dx}=0 \quad ; \quad \frac{d^3v(l)}{dx^3}+k^2\frac{dv(l)}{dx}=0 \quad ; \quad k^2=\frac{P}{EI} \tag{52}$$

where α and β are the parameters quantifying the beam bending stiffness that is retaining the rotations θ_1 or θ_2 at top of each column. The value of this parameter is obtained by using the FEM solution as shown next. For that reason, we refer this development as semi-analytic solution.

Namely, by using the finite element method solution based upon the Hermite polynomials (see Section 3.2) representing the beam deformed shape. We note in passing that such approximation is exact for pure bending of beam with homogeneous cross-section with all loads applied at the nodes, but not for critical mode where deformed shape can be represented by trigonometric functions (e.g., Timoshenko and Gere 1961). We can obtain the following approximation of beam bending contribution to critical mode

$$\begin{pmatrix} M_1 \\ M_2 \end{pmatrix} = \begin{bmatrix} \frac{4EI}{l} & \frac{2EI}{l} \\ \frac{2EI}{l} & \frac{4EI}{l} \end{bmatrix} \begin{pmatrix} \theta_1 \\ \theta_2 \end{pmatrix} = \begin{pmatrix} \frac{6EI}{l} \\ \frac{6EI}{l} \end{pmatrix} \theta \tag{53}$$

which indicates the correct value for parameters $\alpha = 6EI/l$ and $b = a/EI = 6$.

With these boundary conditions we can obtain the critical load by following the usual procedure and enforcing the cero the value of the corresponding determinant

$$\underbrace{\begin{bmatrix} 0 & 1 & 0 & 1 \\ k & 0 & 1 & 0 \\ 0 & 0 & k^2 & 0 \\ (k\beta\cos kl & (-k\beta\sin kl & \beta & 0 \\ -k^2\sin kl) & -k^2\cos kl) & & \end{bmatrix}}_{det[\cdot]=0} \begin{bmatrix} A_1 \\ A_2 \\ A_3 \\ A_4 \end{bmatrix} = \begin{bmatrix} 0 \\ 0 \\ 0 \\ 0 \end{bmatrix} \tag{54}$$

which allows us to obtain the critical load solution as follows

$$k = \sqrt{\frac{P}{EI}} \rightarrow P_{cr} = \frac{(2{,}71)^2\, EI}{l^2} = \frac{7{,}344EI}{l^2} \tag{55}$$

We can see that such a semi-analytic solution is slightly lower than the critical load that we obtain with the FEM approximation of deformed shape by Hermite polynomials used the whole frame (beam and columns); which is equal to

$$P_{cr} = \frac{7{,}5EI}{l^2} \tag{56}$$

That is why we seek the analytic solution wherever possible to get the best estimate of the critical load and to validate our FEM solutions.

In numerical simulation to follow, we propose three different frames (see Fig. 7) each loaded with two compressive conservative or non-conservative loads. The main difference among three

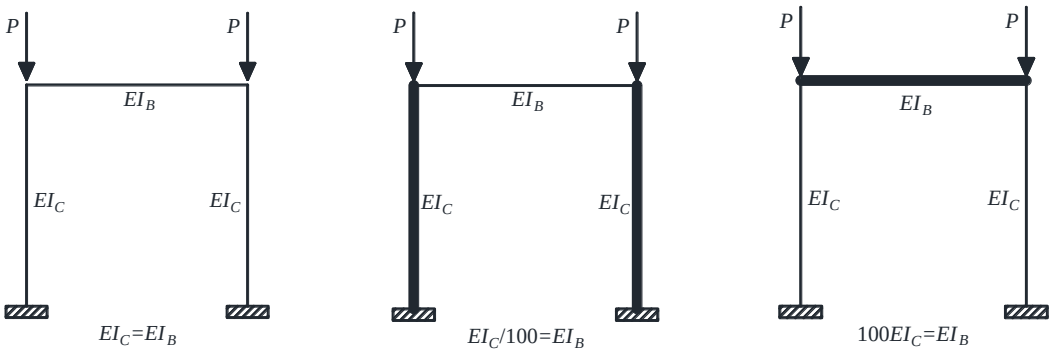

(a) Case 1 (b) Case 2 (c) Case 3

Fig. 7 Different stiffness cases of the frame structure

cases are changing values of the beam bending stiffness *EI*: *i*) the same bending stiffness *EI* in columns and beam, *ii*) the beam bending stiffness is 1/100 of the bending stiffness for columns, *iii*) the beam bending stiffness 100 times bigger than the bending stiffness for columns.

The corresponding analytic solution for each case 2 or 3 can be easily identified from the semi-analytic solution frame value defined in Eq. (55).

Case 2: In this case the contribution of the beam to column tip rotation is very small. In order to define the behavior of the columns, we can neglect the contribution of the beam. Therefore, the value of the critical load tends to the value we already computed for a single cantilever $P_{cr} = 2.05\pi^2 EI/l^2$.

Case 3: In this case the stiffness of the beam is so dominant over the stiffness of the columns that it does not allow any rotation at the top of the columns. This results with the follower load acting as a conservative load. Therefore, the solution is $P_{cr} = \pi^2 EI/(2l)^2$

3. Weak form based solution by finite element method

Since the follower force instability of cantilever cannot be solved using statics approach (Bolotin 1963), we here construct the corresponding dynamics framework. In particular, in this section we will show how such dynamics framework can be generalized to more complex problems that can be solved by using the finite element method. In constructing the weak form solution, the key role is played by von Karman type of strain measure. In our previous work (Ibrahimbegovic *et al*. 2013, Hajdo *et al*. 2020), the von Karman strain was used for formulating instability problems as linear buckling analysis of structures, which reduces to solving the linear eigenvalue problem. Here, we carry on further to introduce the Euler-Bernoulli beam with the von Karman strain measure, as the model capable of accounting for geometric nonlinearities. We will also add the special finite element that can take into account the follower force as the source of instability.

3.1 Variational formulation with von Karman strain as generalization of Euler buckling approach

If we consider for example an axially compressed beam, the strong form of the problem can be written for the case of small deformations and moderate rotations as

$$\frac{d^4 v}{dx^4} + \frac{P}{EI}\frac{d^2 v}{dx^2} = 0 \tag{57}$$

where v is transverse displacement, P is compressive force, E is Young's modulus and I is moment of inertia of beam's cross section. By solving this differential equation, we obtain the Euler critical buckling force. Unfortunately, such a result can only be obtained for simple problems; if one wants to solve more complex problems, we have to employ the weak form, or virtual work (e.g., Ibrahimbegovic 2009). The key role here is played by virtual von Karman strain constructed under hypothesis that deformations are small and rotations are moderate. Under such hypothesis the von Karman deformation measure can be defined for the Euler-Bernoulli beam as follows

$$\varepsilon^{vK} = \frac{du}{dx} + \frac{1}{2}\left(\frac{dv}{dx}\right)^2 - y\frac{d^2 v}{dx^2} \tag{58}$$

By introducing virtual displacements $(\hat{u}, \hat{v})$ to produce the perturbed configuration of the beam deformed configuration, we can apply the Gâteaux derivative in the direction of these virtual displacements to obtain the virtual von Karman deformation

$$\hat{\varepsilon}^{vK} = \frac{d\hat{u}}{dx} + \frac{dv}{dx}\frac{d\hat{v}}{dx} - y\frac{d^2\hat{v}}{dx^2} \tag{59}$$

With this result in hand we can further write the virtual work of internal forces

$$\delta\Pi_{int} = \int_l \int_A \hat{\varepsilon}^{vK} \sigma dA dx = \int_l \left(\frac{d\hat{u}}{dx} N + \frac{d^2\hat{v}}{dx^2} M \right) dx + \int_l \frac{d\hat{v}}{dx}\frac{dv}{dx} N dx \tag{60}$$

The beam stress resultants in terms of axial force N and bending moment M are given as

$$N(x) = EA\frac{du}{dx} \quad ; \quad M(x) = EI\frac{d^2v}{dx^2} \tag{61}$$

We note that the values of stress resultants N and M are obtained from linear theory. Further, we can write an explicit form of the principle of the virtual work or the variational equation

$$\int_l \frac{d\hat{u}}{dx} EA \frac{du}{dx} dx + \int_l \frac{d^2\hat{v}}{dx^2} EI \frac{d^2v}{dx^2} dx + \int_l \frac{d\hat{v}}{dx}\frac{dv}{dx} N dx = \hat{u} f^{ext} \tag{62}$$

where f^{ext} is an external force. The latter is the basis for the approximate solution of instability problem, which can be obtained by the finite element method (Ibrahimbegovic 2009), for a structure of arbitrary complexity.

3.2 Finite element discrete approximation for thin beam and for thick beams

To define the finite element approximation, we will first use a two-node Euler-Bernoulli beam element. In 2D case, each node has three degrees of freedom, two translations and one rotation. The nodal values of the real and virtual displacements are denoted as

$$\begin{aligned} \mathbf{d} &= [u_1 \quad v_1 \quad \varphi_1 \quad u_2 \quad v_2 \quad \varphi_2] \\ \hat{\mathbf{d}} &= [\hat{u}_1 \quad \hat{v}_1 \quad \hat{\varphi}_1 \quad \hat{u}_2 \quad \hat{v}_2 \quad \hat{\varphi}_2] \end{aligned} \tag{63}$$

The real displacement field interpolation is given as

$$\begin{aligned} u(x) &= N_1(x)u_1 + N_2(x)u_2 \\ v(x) &= H_1(x)v_1 + H_2(x)\varphi_1 + H_3(x)v_2 + H_4(x)\varphi_4 \end{aligned} \tag{64}$$

In Eq. (64) above, N_i are the linear shape functions, and H_j are the Hermite cubic polynomials

$$\begin{aligned} N_1(x) &= 1 - \frac{x}{l} & N_2(x) &= \frac{x}{l} \\ H_1(x) &= 1 - 3\left(\frac{x}{l}\right)^2 + 2\left(\frac{x}{l}\right)^3 & H_2(x) &= x - 2\frac{x^2}{l} + \frac{x^3}{l^2} \\ H_3(x) &= 3\left(\frac{x}{l}\right)^2 - 2\left(\frac{x}{l}\right)^3 & H_4(x) &= -\frac{x^2}{l} + \frac{x^3}{l^2} \end{aligned} \tag{65}$$

where l is the length of the beam element. The same kind of interpolation given in Eq. (64) is chosen for the virtual displacement field. The derivatives of the shape functions, and the corresponding deformations can then easily be obtained as follows

$$\frac{du}{dx}(x)=\sum_{a=1}^{2}\frac{dN_a}{dx}u_a=\bar{\mathbf{N}}\mathbf{d}\quad;\quad \frac{d\hat{u}}{dx}(x)=\sum_{a=1}^{2}\frac{dN_a}{dx}\hat{u}_a=\hat{\mathbf{d}}^T\bar{\mathbf{N}}^T\quad;$$
$$\bar{\mathbf{N}}=\begin{bmatrix}\frac{dN_1}{dx} & 0 & 0 & \frac{dN_2}{dx} & 0 & 0\end{bmatrix} \tag{66}$$

We can further obtain the first and the second derivative of the transverse displacement

$$\frac{dv}{dx}(x)=\bar{\mathbf{H}}\mathbf{d}\quad;\quad \frac{d\hat{v}}{dx}(x)=\hat{\mathbf{d}}^T\bar{\mathbf{H}}^T\quad;$$
$$\bar{\mathbf{H}}=\begin{bmatrix}0 & \frac{dH_1}{dx} & \frac{dH_2}{dx} & 0 & \frac{dH_3}{dx} & \frac{dH_4}{dx}\end{bmatrix} \tag{67}$$

$$\frac{d^2v}{dx^2}(x)=\mathbf{B}\mathbf{d}\quad;\quad \frac{d^2\hat{v}}{dx^2}(x)=\hat{\mathbf{d}}^T\mathbf{B}^T\quad;$$
$$\mathbf{B}=\begin{bmatrix}0 & \frac{d^2H_1}{dx^2} & \frac{d^2H_2}{dx^2} & 0 & \frac{d^2H_3}{dx^2} & \frac{d^2H_4}{dx^2}\end{bmatrix} \tag{68}$$

By replacing these results into the relation given in Eq. (62), we can finally obtain the beam internal force as well as the material and the geometric part of the stiffness matrix.

$$f^{int}=\hat{\mathbf{d}}^T\underbrace{\int_l\left(\bar{\mathbf{N}}^T EA\bar{\mathbf{N}}+\mathbf{B}^T EI\mathbf{B}\right)dx}_{\mathbf{K}_m}\mathbf{d}+\hat{\mathbf{d}}^T\underbrace{\int_l\bar{\mathbf{H}}^T\bar{\mathbf{H}}N dx}_{\mathbf{K}_g}\mathbf{d} \tag{69}$$

We note that the tangent stiffness matrix consists of material and geometric matrices

$$\mathbf{K}_t=\mathbf{K}_m+\mathbf{K}_g\quad;$$
$$\mathbf{K}_m=\int_l\left(\bar{\mathbf{N}}^T EA\bar{\mathbf{N}}+\mathbf{B}^T EI\mathbf{B}\right)dx\quad;\quad \mathbf{K}_g=\int_l\bar{\mathbf{H}}^T\bar{\mathbf{H}}N dx \tag{70}$$

To take into account the shear deformation, we modify the material stiffness matrix, as shown in our previous work (Medic *et al*. 2013). More precisely, the entries of the material stiffness matrix are multiplied using shear stiffness proportional coefficients

$$\bar{k}_{22}=-\bar{k}_{25}=-\bar{k}_{52}=-\bar{k}_{55}=\frac{1}{1+\phi}\;;$$
$$\bar{k}_{23}=\bar{k}_{26}=\bar{k}_{32}=\bar{k}_{62}=\bar{k}_{53}=\bar{k}_{56}=\bar{k}_{35}=\bar{k}_{65}=\frac{1}{1+\phi}\;;$$
$$\bar{k}_{33}=\bar{k}_{66}=\frac{1+0.25\cdot\phi}{1+\phi}\;;$$
$$\bar{k}_{36}=\bar{k}_{63}=\frac{1-0.50\cdot\phi}{1+\phi}\;; \tag{71}$$

with ϕ as shear/bending stiffness ratio defined as

$$\phi = \frac{12EI}{kGAl^2} \tag{72}$$

where A is the cross-section area, I moment of inertia, l is element length, E elasticity modulus, G shear modulus and k is shear correction factor. An infinite shear correction factor implies negligible transverse shear deformation, and the element recovers the results in agreement with the Euler-Bernoulli beam theory.

Modeling beam dynamics has been subject of many studies (Culver *et al*. 2019). In case when applied load varies in time, the resulting displacements also vary in time. We assume that the nodal velocities and accelerations are approximated in the same way as the nodal displacements in Eq. (64).

$$\begin{aligned} \ddot{u}(x,t) &= N_1(x)\ddot{u}_1(t) + N_2(x)\ddot{u}_2(t) = \mathbf{N}(x)\ddot{\mathbf{d}}(t) \\ \ddot{v}(x,t) &= H_1(x)\ddot{v}_1(t) + H_2(x)\ddot{\varphi}_1(t) + H_3(x)\ddot{v}_2(t) + H_4(x)\ddot{\varphi}_4(t) = \mathbf{H}(x)\ddot{\mathbf{d}}(t) \end{aligned} \tag{73}$$

where $\mathbf{N}(x)$ and $\mathbf{H}(x)$ are the same shape functions as already used in statics

$$\begin{aligned} \mathbf{N} &= \begin{bmatrix} N_1 & 0 & 0 & N_2 & 0 & 0 \end{bmatrix} \\ \mathbf{H} &= \begin{bmatrix} 0 & H_1 & H_2 & 0 & H_3 & H_4 \end{bmatrix} \end{aligned} \tag{74}$$

The equilibrium equation in this case is replaced by equation of motion that is given as

$$\mathbf{M}\ddot{\mathbf{d}} + \mathbf{K}\mathbf{d} = \mathbf{F}(t) \tag{75}$$

Here, the main novelty is the mass matrix that can be obtained as follows

$$M = \rho A \int_0^l \left(\mathbf{N}^T\mathbf{N} + \mathbf{H}^T\mathbf{H} \right) dx \tag{76}$$

where ρ is the mass density.

3.3 Follower force finite element for thin beams

The virtual work of external forces remains as simple as indicated in Eq. (62) when fixed force is applied. However, we have to deal with a special load case described as a follower force. The follower force is tied to a particular cross-section (Ibrahimbegovic and Taylor 2002). The contribution of the follower force applied at the node a to the virtual work principle is

$$G_{ext} = \delta\boldsymbol{\varphi}_a \mathbf{f}_a^{ext} = \delta\boldsymbol{\varphi}_a \boldsymbol{\Lambda}_t \mathbf{p}_0 \tag{77}$$

where $\mathbf{p}_0$ is the initial value of the follower force, and $\boldsymbol{\Lambda}_t$ is the rotation matrix. The rotation matrix in case of the Euler-Bernoulli beam that takes into account von Karman strain measure has the following form

$$\boldsymbol{\Lambda}_t = \begin{bmatrix} 1 & -\dfrac{dv}{dx} & 0 \\ \dfrac{dv}{dx} & 1 & 0 \\ 0 & 0 & 1 \end{bmatrix} \tag{78}$$

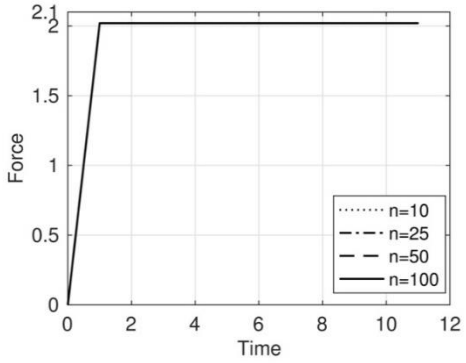

(a) Vertical force - time diagram

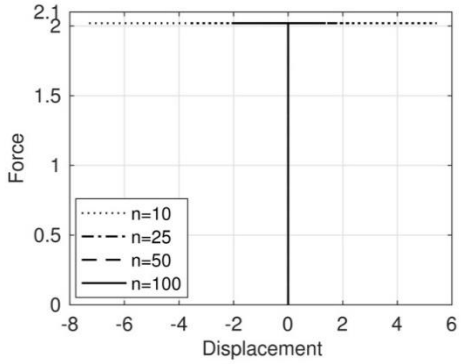

(b) Transverse displacement vertical force diagram indicating instability

Fig. 8 Cantilever instability under follower force

Therefore, the corresponding contribution to the beam element tangent stiffness matrix can be obtained as

$$\mathbf{K}_f = \begin{bmatrix} 0 & 0 & -p_2 \\ 0 & 0 & p_1 \\ 0 & 0 & 0 \end{bmatrix} \tag{79}$$

We note that such contribution to the tangent stiffness has to be applied only to a particular beam element node where the follower force is applied.

4. Numerical examples

4.1 Analysis of a cantilever beam

4.1.1 Cantilever beam under follower force

In first example we study a cantilever beam under follower force P (see Fig. 4). The analytic solution of such problem is presented in Section 2. Hence, this example can provide the validation of our numerical approach.

At the top of the cantilever, we also apply a small horizontal perturbation force of $0.01P$. The chosen material and geometrical properties of the cantilever are as follows: E=10^6 N/cm^2, cross-section area A=1.0cm^2, moment of inertia I=0.001 cm^4, and length is l=100.0 cm. By replacing these values into the analytical solution of the problem, we obtain the critical force value P_{cr}=2.02 N.

We here perform numerical analysis for different number of elements, from 10 to 100. The structure is subjected to the follower force P, and at time of 1 second a small disturbing force is applied to the top of the cantilever. The obtained results are given in Fig. 8.

The analysis performed using our model indeed results with instability phenomena for the analytical value of critical force - 2.02 N. Namely, we can see in Fig. 9, the disproportionally large vibration amplitudes for a small perturbation. The closer we get to analytic solution by using a mesh with 100 elements the instability becomes more visible.

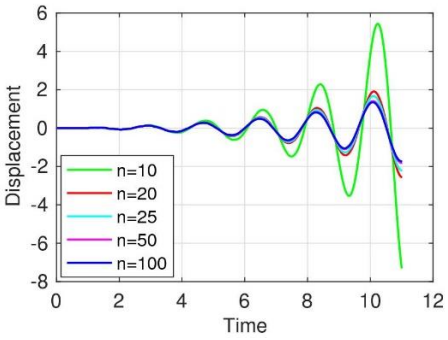

Fig. 9 Cantilever under follower force - time vs transverse displacement

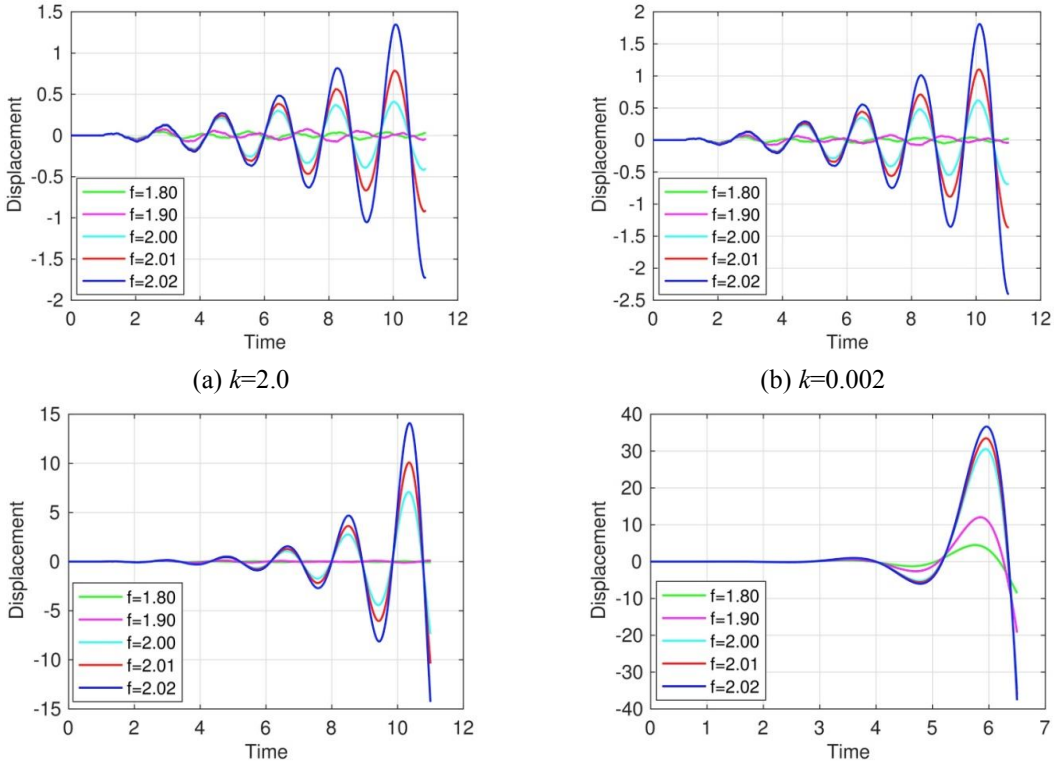

(a) k=2.0 (b) k=0.002

(c) k=0.0002 (d) k=0.00002

Fig. 10 Shear deformation impact to the loss of stability

In Fig. 9, it is shown how dynamic instability develops in time, and how transverse displacement at the free end of the cantilever is increasing in time for a small perturbation introduced in time t=1s. First, we see that the disproportionally large vibration takes some time to develop. We also see that to obtain more accurate results, we have to use a refined mesh of 20 or more beam elements.

4.1.2 Cantilever beam under follower force including shear deformation

Here, we will show how shear deformation affects the value of the critical force. The analytic

solution is already given in Section 2.2. We analyze the same kind of cantilever as in the first example, but with possibility to include shear deformation by using the Timoshenko beam model. We take all the same properties, and also the shear modulus equal to G=0.5×E. In Fig. 10, we give the results for four different values of the shear correction coefficient.

We perform analysis with different values for critical load. We can see in Fig. 10 that the higher is the critical load value, the more quickly the instability is manifested. We also see that the presence of shear deformation reduced the value of critical load.

We have already stated that the infinite shear correction factor implies negligible transverse shear deformation, and the obtained results in this case match the Euler-Bernoulli beam results. Fig. 10(a) shows how transverse displacements changes in time for different force values and shear correction factor 2.0. These results are close to the results given in Fig. 9. If we keep increasing the value of the correction factor, these results would match completely. But in cases when shear deformation is not negligible, Figs. 10(b)-(d), the consequence is an increase in transverse displacement for the same critical force value, or an increase in force value which causes the instability.

4.2 Stability analysis of a frame structure

In this section, we analyze the behavior of the frame structure (see Fig. 5) under two vertical

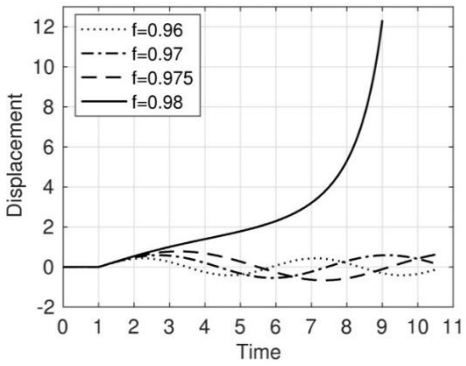

(a) I_{beam}=100×I_{column}

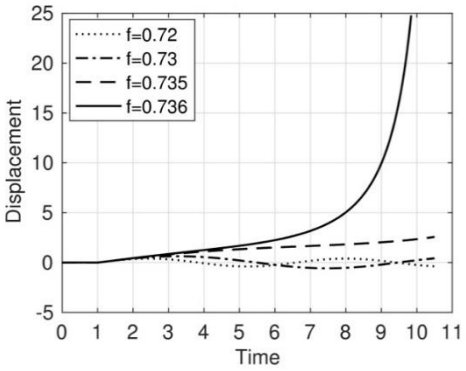

(b) I_{Beam}=I_{column}

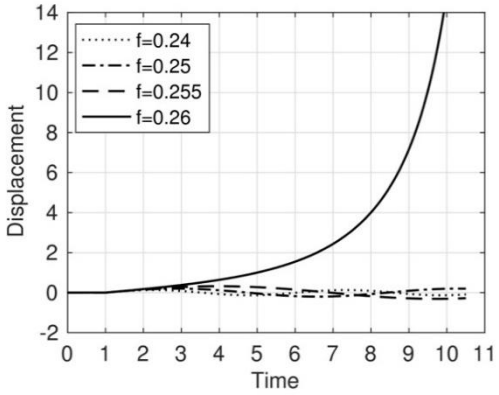

(c) I_{Beam}=0.01×I_{column}

Fig. 11 Frame instability under conservative force

forces P, also loaded with small disturbances in horizontal direction. The horizontal perturbating forces $0.01P$ are applied at the top of the columns. Frame span and height are both equal to l=h=100 cm. Moment of inertia of both columns is I=0.001 cm^4. We perform several analyses varying the beam cross-section properties, while column properties remain constant.

First, we analyze the behavior of the frame under conservative forces, and then we study instability of the frame under nonconservative forces.

4.2.1 Frame under conservative load

In this case we apply two vertical forces, as shown in Fig. 5, and then in time of 1.0 second we apply small horizontal disturbing forces.

The analysis is performed for three cases of beam stiffness: beam moment of inertia equals to columns moment of inertia I_{beam}=I_{column}, beam stiffness is 100 times bigger than stiffness of columns I_{beam}=$100I_{column}$, and finally third analysis is carried out for the case of small beam stiffness I_{beam}=$0.01I_{column}$. In order to obtain the critical force value for all three cases mentioned above, we analyze the stability of the frame due to several different values of vertical forces. The resulting curves are given in Fig. 11. We already gave semi-analytic solution for frame instability in Section 2.3, and now we can compare those results to the results we computed using our beam finite elements. The comparison is summarized in Table 1.

Table 1 Comparison of semi-analytic and numerical solutions for frame critical force

Beam-columns stiffness ratio	Semi-analytic solution	Numerical solution
$I_{beam} = 100I_{column}$	$P_{cr} = 3.14^2 \cdot EI/l^2 = 0.9859$	0.98 N
$I_{beam} = I_{column}$	$P_{cr} = 2.71^2 \cdot EI/l^2 = 0.7344$	0.736 N
$I_{beam} = 0.01I_{column}$	$P_{cr} = 1.57^2 \cdot EI/l^2 = 0.2464$	0.26 N

The results presented in Table 1 show good matching of semi-analytic and numerical solutions for the critical force value of the frame under conservative load.

4.2.2 Frame under follower force

In the third example, we analyze the same frame as in Section 4.2.1, but in this case, we perform instability analysis under two nonconservative follower forces. We also apply small perturbation forces at time of 1 second. Again, we perform several analyses varying the beam cross-section properties, while column properties remain constant.

The results of the analyses are given in Fig. 12. In case when beam moment of inertia is 100 times bigger than the column's moment of inertia, the critical force value is 1.25 N. Note that such a result is in good agreement with the analytical solution for rigid beam (infinite moment of inertia), which gives the value for the critical force equal to 0.98 N.

When columns and beam have the same properties, the instability occurs for the force of 1.55 N. Finally, in case when beam is much weaker than columns, the resulting critical force has value of 2.0 N. When beam moment of inertia tends to zero, the critical force value tends to the analytical solution of the column under follower force.

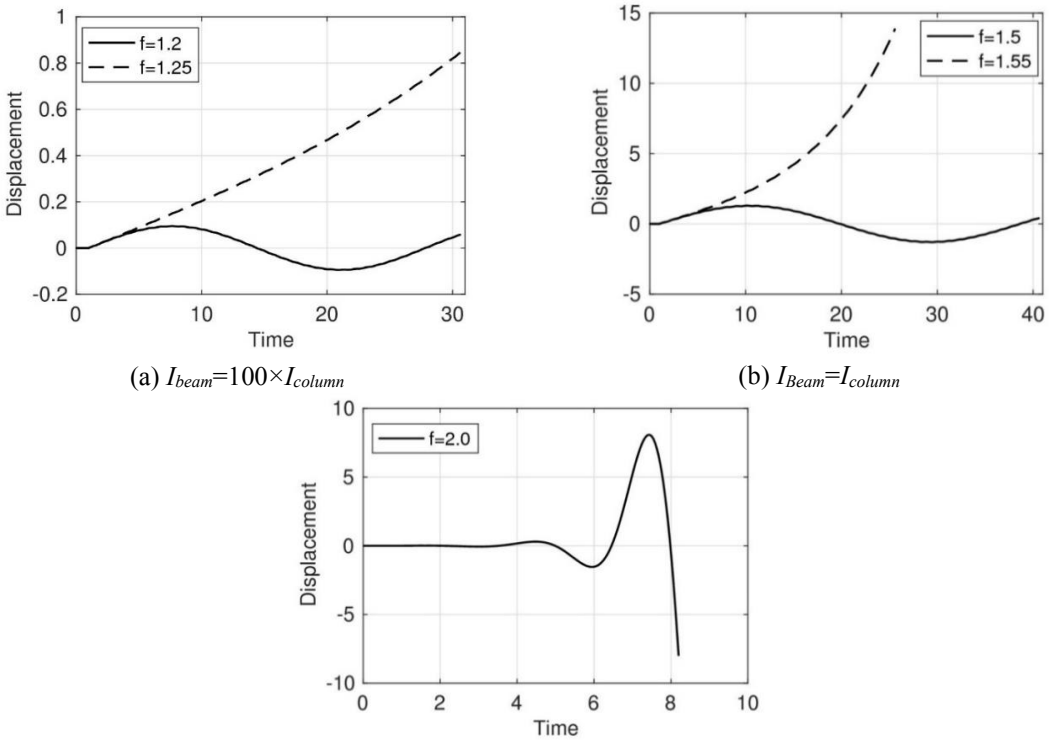

(a) $I_{beam}=100\times I_{column}$ (b) $I_{Beam}=I_{column}$

(c) $I_{Beam}=0.001\times I_{column}$

Fig. 12 Frame under instability under follower force

5. Conclusions

In this paper we deal with instability problems of structures under non-conservative follower force. We demonstrate that the proposed finite element procedure is capable of providing a very efficient analysis for this class of problems considering the structures of any complexity (all those that can be successfully modeled with beam finite elements). We have validated the proposed numerical approach on several examples, including some classical results. Namely, we found out that the solution obtained in the numerical example of cantilever column under follower force shows a very good agreement with the analytic solution for the critical force. After the shear deformation is included, the value of the critical load is reduced, which is also in agreement with the tendencies we should find for this kind of problems.

The stability analysis of frame under follower force indicates that our model can be used in solving even more complex structures. The analysis is performed for several beam-column stiffness ratios. All obtained results are in agreement with available analytic solution.

Acknowledgements

This work was supported by funding from Region HdF (AM), Ministry of Education (EH, II) and IUF (AI). All this support is gratefully acknowledged.

References

Amoozgar, M.R. and Shahverdi, H. (2016), "Dynamic instability of beams under tip follower forces using geometrically exact, fully intrinsic equations", *Lat. Am. J. Solid. Struct.*, **13**, 3022-3038. https://doi.org/10.1590/1679-78253010.

Beck, M. (1952), "Die Knicklast des einseitig eingespannten, tangential gedrückten Stabes", *J. Appl. Math. Phys.*, **3**, 225-228. https://doi.org/10.1007/BF02008828.

Bolotin, V.V. (1963), *Nonconservative Problems of Theory of Elastic Stability*, Pergamon Press.

Bolotin, V.V. (1964), *The Dynamic Stability of Elastic Systems*, Holden-Day Inc.

Brank, B. and Lovrencic, M. (2018), "Simulation of shell buckling by implicit dynamics and numerically dissipative schemes", *Thin Wall. Struct.*, **132**, 682-699. https://doi.org/10.1016/j.tws.2018.08.010.

Culver, D., McHugh, K.A. and Dowell, E.H. (2019), "An assessment and extension of geometrically nonlinear beam theories", *Mech. Syst. Signal Pr.*, **134**, 106340. https://doi.org/10.1016/j.ymssp.2019.106340.

Dujc, J., Brank, B. and Ibrahimbegovic, A. (2010), "Multi-scale computational model for failure analysis of metal frames that includes softening and local buckling", *Comput. Meth. Appl. Mech. Eng.*, **199**(21-22), 1371-1385. https://doi.org/10.1016/j.cma.2009.09.003.

Elishakoff, I. (2005), "Controversy associated with the so-called "Follower Forces": Critical overview", *Appl. Mech. Rev.*, **58**(2), 117-142. https://doi.org/10.1115/1.1849170.

Farhat, C., Kwan-yu Chiu, E., Amsallem, D., Sholte, J. and Ohayon, R. (2013), "Modeling of fuel sloshing and its physical effects on flutter", *AIAA J.*, **51**(9), 100-114. https://doi.org/10.2514/1.J052299.

Fazelzadeh, S.A., Karimi-Nobandegani, A. and Mardanpour, P. (2017), "Dynamic Stability of Pretwisted Cantilever Beams Subjected to Distributed Follower Force", *AIAA J.*, **55**(3), 955-964. https://doi.org/10.2514/1.J055421.

Gasparini, A.M., Saetta, A.V. and Vitaliani, R.V. (1995), "On the stability and instability regions of non-conservative continuous system under partially follower forces", *Comput. Meth. Appl. Mech. Eng.*, **124**, 63-78. https://doi.org/10.1016/0045-7825(94)00756-D.

Hajdo, E., Ibrahimbegovic, A. and Dolarevic, S. (2020), "Buckling analysis of complex structures with refined model built of frame and shell finite elements", *Coupl. Syst. Mech.*, **9**, 29-46. http://dx.doi.org/10.12989/csm.2020.9.1.029.

Ibrahimbegovic, A. (2009), *Nonlinear Solid Mechanics: Theoretical Formulations and Finite Element Solution Methods*, Springer, Berlin, Germany.

Ibrahimbegovic, A. and Taylor, R.L. (2002), "On the role of frame-invariance of structural mechanics models at finite rotations", *Comput. Meth. Appl. Mech. Eng.*, **191**, 5159-5176. https://doi.org/10.1016/S0045-7825(02)00442-5.

Ibrahimbegovic, A., Hajdo, E. and Dolarevic, S. (2013), "Linear instability or buckling problems for mechanical and coupled thermomechanical extreme conditions", *Coupl. Syst. Mech.*, **2**, 349-374. http://dx.doi.org/10.12989/csm.2013.2.4.349.

Imamovic I., Ibrahimbegovic, A. and Hajdo, E. (2019), "Geometrically exact initially curved Kirchhoff's planar elasto-plastic beam", *Coupl. Syst. Mech.*, **8**, 537-553. https://doi.org/10.12989/csm.2019.8.6.537.

Jeronen, J. and Kouhia, R. (2015), "On the effect of damping on stability of nonconservative systems", *Proceedings XII Finish Mechanics Days*, Eds. R. Kouhia *et al*., 77-82.

Lacarbonara, W. and Yabuno, H. (2006), "Refined models of elastic beams undergoing large in-plane motions: theory and experiment", *Int. J. Solid. Struct.*, **43**(17), 5066-5084. https://doi.org/10.1016/j.ijsolstr.2005.07.018.

Langthjem, M.A. and Sugiyama, Y. (2000), "Dynamics stability of column subjected to follower load", *J. Sound Vib.*, **238**(5), 809-851. https://doi.org/10.1006/jsvi.2000.3137.

Lozano, R., Brogliato, B., Egeland, O. and Maschke, B. (2000), *Dissipative Systems Analysis and Control: Theory and Applications*, Springer.

Masjedi, P.K. and Ovesy, H.R. (2015) "Large deflection analysis of geometrically exact spatial beams under conservative and nonconservative loads using intrinsic equations", *Acta Mech.*, **226**, 1689-1706.

https://doi.org/10.1007/s00707-014-1281-3.
McHugh, K.A. and Dowell, E.H. (2020), "Nonlinear response of an inextensible, free-free beam subjected to a nonconservative follower force", *J. Comput. Nonlin. Dyn.*, **15**(2), 021003. https://doi.org/10.1115/1.4045532.
Medic, S., Dolarevic, S. and Ibrahimbegovic, A. (2013), "Beam model refinement and reduction", *Eng. Struct.*, **50**, 158-169. https://doi.org/10.1016/j.engstruct.2012.10.004.
Mejia Nava, A.R., Ibrahimbegovic, A. and Lozano, R. (2020), "Instability phenomena and their control in statics and dynamics: Application to deep and shallow truss and frame structures", *Coupl. Syst. Mech.*, **9**, 47-62. http://dx.doi.org/10.12989/csm.2020.9.1.047.
Piculin, S. and Brank, B. (2015), "Weak coupling of shell and beam computational models for failure analysis of steel frames", *Finite Elem. Anal. Des.*, **97**, 20-42. https://doi.org/10.1016/j.finel.2015.01.001.
Sugiyama, Y., Langthjem, M.A. and Katayama, K. (2019), *Dynamic Stability of Columns under Nonconservative Forces: Theory and Experiment*, Springer.
Timoshenko, S. and Gere, J.M. (1961), *Theory of Elastic Stability*, McGraw Hill.

AI